COMPUTATIONAL & APPLIED MATHEMATICS

Volume 30, N. 2, pp. 399–425, 2011

ISSN 0101-8205
www.scielo.br/cam

Relaxation approaches to the optimal control of the Euler equations

JEAN MEDARD T. NGNOTCHOUYE[1]*, MICHAEL HERTY[2], SONJA STEFFENSEN[3] and MAPUNDI K. BANDA[4]

[1]School of Mathematical Sciences, University of KwaZulu-Natal, Private Bag X01, Scottsville 3209, Pietermaritzburg, South Africa
[2]RWTH University Aachen, Templergraben 55, D-52056 Aachen, Germany
[3]RWTH University Aachen, Templergraben 55, D-52056 Aachen, Germany
[4]School of Computational and Applied Mathematics, University of the Witwatersrand, Private Bag 3, Wits 2050, South Africa

E-mails: Ngnotchouye@ukzn.ac.za / herty@mathc.rwth-aachen.de / steffensen@mathc.rwth-aachen.de / Mapundi.Banda@wits.ac.za

Abstract. The treatment of control problems governed by systems of conservation laws poses serious challenges for analysis and numerical simulations. This is due mainly to shock waves that occur in the solution of nonlinear systems of conservation laws. In this article, the problem of the control of Euler flows in gas dynamics is considered. Numerically, two semi-linear approximations of the Euler equations are compared for the purpose of a gradient-based algorithm for optimization. One is the Lattice-Boltzmann method in one spatial dimension and five velocities (D1Q5 model) and the other is the relaxation method. An adjoint method is used. Good results are obtained even in the case where the solution contains discontinuities such as shock waves or contact discontinuities.

Mathematical subject classification: Primary: 49Mxx; Secondary: 65Mxx.

Key words: Lattice Boltzmann method, relaxation methods, adjoint method, optimal control, systems of conservation laws, Euler equations.

#CAM-197/10. Received: 24/III/10. Accepted: 30/IX/10.
*Corresponding author.

1 Introduction

In this paper, numerical approaches for optimization problems governed by nonlinear systems of hyperbolic conservation laws are considered. More precisely, the investigation of optimal control problems subject to the dimensionless one-dimensional Euler system in conservative variables [1]

$$\mathbf{u}(x,t) = (\rho,\, \rho u,\, \rho(b\theta + u^2))(x,t)$$

given as

$$\partial_t \rho + \partial_x (\rho u) = 0, \tag{1a}$$

$$\partial_t (\rho u) + \partial_x \left(\rho u^2 + p\right) = 0, \tag{1b}$$

$$\partial_t \left(\rho \left(b\theta + u^2\right)\right) + \partial_x \left(\rho u \left(b\theta + u^2\right) + 2pu\right) = 0, \tag{1c}$$

where t is the time, x is the spatial coordinate, ρ, u, θ and

$$p = \rho\theta$$

are the density, the flow velocity in the x direction, the temperature, and the pressure of a gas, respectively. The constant $b = \frac{2}{\gamma - 1}$ with γ the specific heat ratio. The initial conditions are

$$\mathbf{u}_0 = \left(\rho_0,\, \rho_0 u_0,\, \rho_0\left(b\theta_0 + (u_0)^2\right)\right) \quad \text{at} \quad t = 0, \tag{2}$$

where ρ_0, u_0, and θ_0 are the given initial density, velocity and temperature, respectively, as functions of the spatial variable x. This form of the Euler equation is applied in order to be consistent with the lattice Boltzmann equation as studied in [1]. Here the main interest is the computation of optimal initial values $\mathbf{u}_0 = \mathbf{u}(x,0)$ which match a given desired state $\mathbf{u}_d$ at time T. The problem is formulated as

$$\min_{\mathbf{u}_0} \mathcal{J}(\mathbf{u}(\cdot, T), \mathbf{u}_0; \mathbf{u}_d) \text{ subject to equation (1) and } \mathbf{u}(x, t = 0) = \mathbf{u}_0(x). \tag{3}$$

It is known that in general the semi-group generated by a conservation law is non-differentiable in L^1 even in the scalar, one-dimensional case. A differential structure on general BV-solutions for hyperbolic conservation laws in one space dimension has been introduced and discussed in [2, 3, 4, 5, 6]. Based on the

derived calculus, first-order optimality conditions for systems have been given in [7]. Theoretical discussion on the resulting non-conservative equations can be found in [8, 9, 10]. Numerical results in the scalar, one-dimensional case with distributed control are also presented in [11, 6, 12]. Work on advection equations has been presented in [13]. For time integration of optimal control problems, Runge-Kutta schemes have been developed in [17]. In general, it can be observed that the shock waves that occur in the solution of nonlinear systems of conservation laws pose a challenge [26, 2, 3, 4, 5, 6, 11, 12].

More recently alternative approaches for developing computational approaches for optimization problems governed by nonlinear conservation laws based on adjoint methods have appeared in the literature [26, 15, 14, 16]. These methods have also been applied to flow models which develop discontinuities in flow variables, for example, shock waves [26]. Optimal control problems governed by scalar conservation laws were presented in [26] and specifically for the inviscid one-dimensional Burgers equation in [14]. Also an adjoint formulation for the optimization of viscous flows suitable for both structured and unstructured grids was presented in [15]. Shape optimization of aerodynamic problems in which a two-dimensional system is governed by the steady Euler equations were also presented in [16].

The Lattice Boltzmann method (LBM) which is a discretisation of the Lattice Boltzmann Equations (LBE) has been applied extensively to solve problems in fluid dynamics. For more details the reader is referred to [20, 19] and the references therein. The application of the method for the approximation of the Euler equations was proposed in [1]. The solution of optimization problems in computational fluid dynamics using the LBM has been presented in [27] where problems of shape optimization and topology optimization were considered and the sensitivity method used. The macroscopic models were the incompressible Navier-Stokes equations [28, 29].

The aim of this paper is to contribute to the development of numerical approaches for solving optimization problems based on the adjoint method. The main focus of this paper is to develop simple and efficient numerical approaches for optimization problems governed by hyperbolic equations. Instead of applying the nonlinear hyperbolic problems directly, semi-linear problems with linear flux functions and stiff non-linear source terms are derived. In this framework

the hyperbolic structure of the constraints is preserved in the asymptotic limit at the additional expense of increasing the number of equations and introducing additional source terms (relaxation terms). Two relaxation approaches are considered: the Lattice-Boltzmann equations (LBE) [18, 19, 1, 20] and the so called relaxation approximations [21, 22, 23]. For the latter, strong-stability preserving (SSP) [24] as well as asymptotic-preserving Implicit-Explicit (IMEX) schemes are applied for time integration of the hyperbolic systems with stiff source terms [25]. For such relaxation systems, the adjoint equation is derived. Moreover, the optimal flow variables are obtained at the hydrodynamic limit as the Knudsen number goes to zero. The properties of the relaxation schemes applied to optimization problems have been discussed in [26] for scalar nonlinear problems. Therefore, in Section 3 a brief presentation of the method based on relaxation approaches will be given. The formulation of the optimal control problem as an optimization problem with partial differential equations is presented in Section 2. The partial differential equations (PDE) are replaced with either their kinetic approximation formulated as LBEs or their relaxation approximation in the form of a relaxation system. A brief discussion on the relaxation method for the control of systems of conservation laws is presented in Section 3. Thereafter the Euler equations and their approximation using a Lattice Boltzmann formulation are presented in Section 4. Moreover in this section, a brief discussion on the convergence of the kinetic model towards the hydrodynamic model is discussed, see also [1] for a detailed presentation. The derivation of the adjoint calculus at the kinetic level is presented in Section 4.1. The numerical formulation of the optimization problem as well as some numerical tests on practical problems of interest are documented in Section 5. Finally, concluding remarks and future extensions are presented in Section 6.

2 Problem formulation

An optimization problem of the form

$$\underset{\mathbf{u}_0}{\text{Minimize}}\ \mathcal{J}(\mathbf{u}(\cdot, T), \mathbf{u}_0; \mathbf{u}_d) = \frac{1}{2}\int_{\mathbb{R}} \|\mathbf{u}(x, T) - \mathbf{u}_d(x)\|^2 dx, \tag{4}$$

where $\mathbf{u} = (\rho, \rho u, \rho(b\theta + u^2))$ is the solution to the Euler equations (1) with initial data $\mathbf{u}_0$ is considered. In (4), $\mathbf{u}_d$ represents a desired state that needs to be

approximately attained at time $t = T$ and $\mathcal{J}(\mathbf{u}(\cdot, T), \mathbf{u}_0; \mathbf{u}_d)$ is a cost functional of the tracking type in the form

$$\begin{aligned}\mathcal{J}(\mathbf{u}(\cdot, T), \mathbf{u}_0; \mathbf{u}_d) &= \frac{1}{2}\int_{\mathbb{R}} \|\mathbf{u}(x, T) - \mathbf{u}_d(x)\|^2 dx \\ &= \frac{1}{2}\int_{\mathbb{R}} \Big[\big(\rho(x, T) - \rho_d(x)\big)^2 + \big(m(x, T) - m_d(x)\big)^2 \\ &\quad + \big(E(x, T) - E_d(x)\big)^2 dx\Big]\end{aligned} \tag{5}$$

where the momentum is denoted as $m = \rho u$ and the energy as $E = \rho(b\theta + u^2)$.

The solution of the optimal control problem (4) poses problems in practice due to shock waves that can occur in the solution of the flow equation (1) [30, 26]. To overcome these problems, two semi-linear approximations of the Euler equations (1) namely the Lattice Boltzmann approximation and the relaxation approximation are applied.

3 Relaxation method for the control of the Euler equation

In [23] a relaxation system was introduced for the derivation of numerical schemes to approximate a general nonlinear conservation law [21, 22]. A way to apply hyperbolic relaxation in the case of a scalar conservation law has been described in [26] and only a brief summary of the application of the relaxation method for solving problem (3) will be presented here. To simplify the notation, the nonlinear flux will be denoted by $\mathbf{f} : \mathbb{R}^3 \to \mathbb{R}^3$ and given as

$$f(\mathbf{u}) = \begin{bmatrix} m \\ \frac{E}{b} + \frac{m^2(b-1)}{b\rho} \\ \frac{mE}{\rho} + \frac{2m(\rho E - m^2)}{b\rho^2} \end{bmatrix}. \tag{6}$$

Then, problem (3) is

$$\min_{\mathbf{u}_0} \mathcal{J}(\mathbf{u}(\cdot, T), \mathbf{u}_0; \mathbf{u}_d) \quad \text{subject to} \quad \partial_t \mathbf{u} + \partial_x \mathbf{f}(\mathbf{u}) = 0,\ \mathbf{u}(x, 0) = \mathbf{u}_0 \tag{7}$$

where $\mathbf{u}_d$ is the desired state. The relaxation approximation to the optimization problem (7) reads

$$\min_{u_0} \mathcal{J}(\mathbf{u}(\cdot, T), \mathbf{u}_0; \mathbf{u}_d) \quad \text{subject to} \begin{cases} \partial_t \mathbf{u} + \partial_x \mathbf{v} = 0, \\ \partial_t \mathbf{v} + \mathbf{A}^2 \partial_x \mathbf{u} = \frac{1}{\tau}\left(\mathbf{f}(\mathbf{u}) - \mathbf{v}\right), \\ \mathbf{u}(x, 0) = \mathbf{u}_0,\ \mathbf{v}(x, 0) = \mathbf{f}(\mathbf{u}_0), \end{cases} \tag{8}$$

where $\tau > 0$ is the relaxation rate and

$$\mathbf{A} = \mathrm{diag}(a_1, a_2, a_3) \in \mathbb{R}^{3\times 3}$$

is a given diagonal matrix satisfying the subcharacteristic condition

$$\max_{\mathbf{u}} \|\lambda_k(D\mathbf{f}(\mathbf{u}))\| \leq a_k \tag{9}$$

and λ_k denotes the k-th eigenvalue of the Jacobian matrix $D\mathbf{f}(\mathbf{u})$. The approximation of the conservation law by (8) has a linear transport part combined with a stiff source term. The characteristic variables of the transport part are $\mathbf{v} \pm \mathbf{Au}$. In the small relaxation limit, $\tau \to 0$, one obtains, to leading order, $\mathbf{v} = \mathbf{f}(\mathbf{u}) + O(\tau)$. The numerical discretization is done without using Riemann solvers and originally a first order Upwind scheme and a second order MUSCL scheme together with a second-order TVD implicit-explicit (IMEX) time integration scheme has been discussed. The schemes are used in the regime $\tau \ll \Delta x$.

Using a formal Lagrangian approach the linear adjoint equations to (8) are derived as

$$\begin{aligned} -\partial_t \mathbf{p} - \mathbf{A}^2 \partial_x \mathbf{q} &= \frac{1}{\tau} D\mathbf{f}(\mathbf{u})^T \mathbf{q}, & \mathbf{p}(x, t = T) &= \mathbf{p}_T(x), \\ -\partial_t \mathbf{q} - \partial_x \mathbf{p} &= -\frac{1}{\tau}\mathbf{q}, & \mathbf{q}(x, t = T) &= \mathbf{q}_T(x). \end{aligned}$$

See also [26] for a more detailed presentation for scalar equations. An expansion in terms of τ yields the solution $(\mathbf{p}, \mathbf{q})$ which solves the following second-order equation

$$-\mathbf{p}_t - D\mathbf{f}(\mathbf{u})^T \mathbf{p}_x = \tau \mathbf{A}^2 \mathbf{p}_{xx}.$$

In [26] the validity of the formal computations in the scalar case has been shown in view of the approximation of the solution to the minimization problem (7) and the solution to the relaxation system (8). It can be shown that the discrete numerical scheme in the limit $\tau \to 0$ converges to the continuous adjoint equation. Furthermore, in the case of a first-order spatial discretization, convergence to the optimality system for the discretized system is obtained. The relaxation approximation will be extended to systems and comparisons with the adjoint calculus derived for the Lattice-Boltzmann approximations will be made.

Using the cost functional in equation (6) and hence solving, numerically, the formal first-order optimality system takes the form:

$$
\begin{aligned}
&\partial_t \mathbf{u} + \partial_x \mathbf{v} = 0, && \mathbf{u}(x,0) = \mathbf{u}_0,\\
&\partial_t \mathbf{v} + \mathbf{A}^2 \partial_x \mathbf{u} = \frac{1}{\tau}\left(\mathbf{f}(\mathbf{u}) - \mathbf{v}\right), && \mathbf{v}(x,0) = \mathbf{f}(\mathbf{u}_0),\\
&-\partial_t \mathbf{p} - \mathbf{A}^2 \partial_x \mathbf{q} = \frac{1}{\tau} D\mathbf{f}(\mathbf{u})^T \mathbf{q}, && \mathbf{p}(x, t=T) = \mathbf{u}(x, t=T) - \mathbf{u}_d(x),\\
&-\partial_t \mathbf{q} - \partial_x \mathbf{p} = -\frac{1}{\tau}\mathbf{q}, && \mathbf{q}(x, t=T) = 0,\\
&\mathbf{p}(x,0) + D\mathbf{f}(\mathbf{u}_0)\mathbf{q}(x,0) = 0;
\end{aligned}
$$

where $\mathbf{f}$ is given by the flux of Euler's system. For forward and adjoint equations, similar discretizations as in the scalar case in [26], are used.

4 A kinetic approximation of the Euler equation

In this section, the Lattice Boltzmann approximation of the Euler equation proposed in [1] is adapted.

A Lattice-Boltzmann approximation to the compressible Euler equations (1) is described as follows. Let ξ_i, where $i \in \{0, \ldots, N-1\}$, be the molecular velocity in the x direction of the i-th particle, with N the total number of molecular velocities. The variable η_i is also introduced – its role will be discussed later. The velocity distribution function of the i-th particle is denoted by $f_i(x,t)$. The macroscopic variables ρ, u and θ are defined as

$$
\rho = \sum_{i=0}^{N-1} f_i, \quad m = \sum_{i=0}^{N-1} \xi_i f_i \quad \text{and} \quad \rho(b\theta + u^2) = \sum_{i=0}^{N-1} (\xi_i^2 + \eta_i^2) f_i. \tag{10}
$$

Now the initial-value problem for the kinetic equation is considered:

$$
\frac{\partial f_i}{\partial t} + \xi_i \frac{\partial f_i}{\partial x} = \Omega_i(f), \quad i \in \{0, \ldots, N-1\} \tag{11}
$$

where the collision operator, $\Omega_i(f)$, with $f = (f_0, \ldots, f_{N-1})$, is of the Bhatnagar-Gross-Krook (BGK)-type [31]

$$
\Omega_i(f) = \frac{f_i^{eq}(\rho, m, E) - f_i}{\varepsilon}. \tag{12}
$$

Therein $\varepsilon = \frac{\mu\sqrt{R\theta_0}}{L}$ is the *Knudsen number*, μ the *relaxation time*, R is the specific gas constant, L, θ_0 a reference length and a reference temperature, respectively, and $f_i^{eq}(\rho, m, E)$ is the local equilibrium distribution depending on the macroscopic variables. The initial conditions are given by

$$f_i = f_i^{eq}(\rho_0, m_0, E_0) \quad \text{at} \quad t = 0. \tag{13}$$

One can integrate the LBE (11) along characteristics to obtain the classical form of the Lattice Boltzmann method (LBM) [20]. Alternatively, other finite volume approaches can be applied [32, 23]. To derive a general form for the adjoint calculus for the optimization problem, the general form (11) is considered. To recover the Euler equation at the hydrodynamic limits from the Lattice Boltzmann equation, the following constraints are imposed on the moments of the local equilibrium distribution f_i^{eq} [1]

$$\sum_{i=0}^{N-1} f_i^{eq} = \rho, \tag{14a}$$

$$\sum_{i=0}^{N-1} f_i^{eq}\xi_i = \rho u, \tag{14b}$$

$$\sum_{i=0}^{N-1} f_i^{eq}\xi_i^2 = p + \rho u^2, \tag{14c}$$

$$\sum_{i=0}^{N-1} f_i^{eq}(\xi_i^2 + \eta_i^2) = \rho(b\theta + u^2). \tag{14d}$$

It has to be noted here that the collision term conserves mass, momentum and energy. Hence the distribution functions must also be constrained by

$$\sum_{i=0}^{N-1} f_i = \rho, \tag{15a}$$

$$\sum_{i=0}^{N-1} f_i\xi_i = \rho u, \tag{15b}$$

$$\sum_{i=0}^{N-1} f_i(\xi_i^2 + \eta_i^2) = \rho(b\theta + u^2). \tag{15c}$$

From now on, the D1Q5 Lattice Boltzmann model for a system with one-dimension and five molecular velocities will be discussed. The exact form of the discrete velocities are given as in [1]

$$\xi_i = \begin{cases} 0, & \text{for } i = 0; \\ \nu_1 \cos[(i-1)\pi], & \text{for } i = 1, 2; \\ \nu_2 \cos[(i-1)\pi], & \text{for } i = 3, 4. \end{cases} \tag{16}$$

The constants η_i are given as

$$\eta_i = \begin{cases} \eta_0, & \text{for } i = 0 \\ 0, & \text{for } i \neq 0. \end{cases} \tag{17}$$

Note that ν_1 and ν_2, with $\nu_2 \neq \nu_1$, and η_0 are given nonzero constants. The equilibrium distribution is given in the form [1]

$$f_i^{eq} = \rho A_i + m\xi_i B_i, \tag{18}$$

where

$$A_i = \begin{cases} \frac{b-1}{\eta_0^2}\theta, & \text{for } i = 0, \\ \frac{1}{2\left(\nu_1^2-\nu_2^2\right)}\left[-\nu_2^2 + \left((b-1)\frac{\nu_2^2}{\eta_0^2}+1\right)\theta + u^2\right], & \text{for } i = 1, 2 \\ \frac{1}{2\left(\nu_2^2-\nu_1^2\right)}\left[-\nu_1^2 + \left((b-1)\frac{\nu_1^2}{\eta_0^2}+1\right)\theta + u^2\right], & \text{for } i = 3, 4; \end{cases} \tag{19a}$$

and

$$B_i = \begin{cases} 0, & i = 0; \\ \frac{-\nu_2^2+(b+2)\theta+u^2}{2\nu_1^2\left(\nu_1^2-\nu_2^2\right)}, & i = 1, 2; \\ \frac{-\nu_1^2+(b+2)\theta+u^2}{2\nu_2^2\left(\nu_2^2-\nu_1^2\right)}, & i = 3, 4. \end{cases} \tag{19b}$$

It can be pointed out here that the LBE, equation (11), converges in the hydrodynamic limit to the Euler equations [1]. The weak solution of the Euler equations (1) satisfies

$$\begin{aligned} \int_0^\infty \int_{\mathbb{R}} \left(\frac{\partial \psi}{\partial t} \begin{Bmatrix} \rho \\ \rho u \\ \rho(b\theta + u^2) \end{Bmatrix} + \frac{\partial \psi}{\partial x} \begin{Bmatrix} \rho \\ \rho u^2 + p \\ \rho u(b\theta + u^2) + 2p\,u \end{Bmatrix} \right) dx\,dt \\ + \int_{\mathbb{R}} \begin{Bmatrix} \rho_0 \\ \rho_0 u_0 \\ \rho_0(b\theta_0 + (u_0)^2) \end{Bmatrix} \psi(x, 0) dx = 0, \end{aligned} \tag{20}$$

where, $\psi(x,t)$ is a smooth test function of x and t which vanishes for $t+|x|$ large enough. To obtain the weak solution of the Euler equation from the kinetic equation system (11), the weak form of the LBE (11) in the form

$$\int_0^\infty \int_{\mathbb{R}} \left(\frac{\partial \psi}{\partial t} + \xi_i \frac{\partial \psi}{\partial x} \right) f_i - \frac{f_i^{eq}(\rho, m, E) - f_i}{\varepsilon} \psi \, dx \, dt + \int_{\mathbb{R}} f_i^{eq}(\rho_0, m_0, E_0) \psi(x,0) dx = 0, \tag{21}$$

where ψ is a test function as above, independent of ε, is considered. In addition, $f_i(x,0) = f_i^{eq}(\rho_0, m_0, E_0)$. It was proven in [1] that the finite difference form of the kinetic equation (11) is consistent with the above integral form (21) even if the mesh width is of order $O(\varepsilon)$. According to the analysis of the Boltzmann equation, shock waves and contact discontinuities are not real discontinuities in the realm of Lattice Boltzmann simulations, but thin layers of width $O(\varepsilon)$ across which the variable makes an appreciable variation [1]:

Proposition 4.1. [1] *Consider a case where the solution f_i contains shocks or contact discontinuities in some region, "the steep region", where the order of variation of f_i in the space and time variable is $O(\varepsilon)$. In other regions which are called Euler regions, f_i has a moderate variation in x and t in the order of unity. Then the solution f_i of* (21) *in the limit $\varepsilon \to 0$ is given by $f_i = f_i^{eq}(\rho, m, E)$ whose macroscopic variable ρ, m, E satisfy the weak form of the Euler equation given by* (20)*.*

For the proof, the reader may refer to [1].

4.1 Derivation of an adjoint system using the LBE

The Lagrangian at the microscopic level is given by

$$\mathcal{L}(f,\lambda) = \mathcal{J}(\mathbf{u}(\cdot,T), \mathbf{u}_0; \mathbf{u}_d) - \sum_{i=0}^{N-1} \int_0^T \int_{\mathbb{R}} \times \left[\partial_t f_i + \xi_i \partial_x f_i - \Omega_i(f) \right] \lambda_i \, dx \, dt, \tag{22}$$

where λ_i are the Lagrange multipliers or the *adjoint velocity distributions*. Integrating the second term on the right hand side of equation (22) by parts, one

obtains

$$\begin{aligned}\mathcal{L}(f,\lambda) \;=\; & \mathcal{J}(\mathbf{u}(\cdot,T),\mathbf{u}_0;\mathbf{u}_d)+\sum_{i=0}^{N-1}\int_0^T\int_{\mathbb{R}} f_i\big[\partial_t\lambda_i+\xi_i\,\partial_x\lambda_i\big]\\ & +\Omega_i(f)\lambda_i\,dx\,dt-\sum_{i=0}^{N-1}\int_{\mathbb{R}}\big(f_i(x,T)\lambda_i(x,T)\\ & -f_i^{eq}(\rho_0(x),m_0(x),E_0(x))\lambda_i(x,0)\big)dx.\end{aligned} \tag{23}$$

By taking the variation of the Lagrangian with respect to the state variable f_i and taking into account (10), the following adjoint system is derived

$$-\partial_t\lambda_i-\xi_i\partial_x\lambda_i=\sum_{j=0}^{N-1}\frac{\partial\Omega_j(f)}{\partial f_i}\lambda_j \tag{24}$$

with a terminal condition

$$\lambda_i(\cdot,T)=\left(\big(\rho(\cdot,T)-\rho_d\big)\frac{\partial\rho}{\partial f_i}+\big(m-m_d\big)\frac{\partial m}{\partial f_i}+\big(E-E_d\big)\frac{\partial E}{\partial f_i}\right), \quad x\in\mathbb{R}, \tag{25}$$

with

$$\frac{\partial\rho}{\partial f_i}=1,\quad \frac{\partial m}{\partial f_i}=\xi_i,\quad \frac{\partial E}{\partial f_i}=\xi_i^2+\eta_i^2. \tag{26}$$

The adjoint equation (24) has the same structure as the original model (11). Thus the term on the right hand side of (24) can be referred to as the *adjoint collision operator*. In the BGK formulation, the adjoint collision operator has the form

$$\sum_{j=0}^{N-1}\frac{\partial\Omega_j(f)}{\partial f_i}\lambda_j=\frac{1}{\varepsilon}\left(\sum_{j=0}^{N-1}\frac{\partial f_j^{eq}}{\partial f_i}\lambda_j-\lambda_i\right). \tag{27}$$

For the equilibrium functional given in (18), one obtains

$$\frac{\partial f_j^{eq}}{\partial f_i}=\frac{\partial f_j^{eq}}{\partial\rho}\frac{\partial\rho}{\partial f_i}+\frac{\partial f_j^{eq}}{\partial m}\frac{\partial m}{\partial f_i}+\frac{\partial f_j^{eq}}{\partial E}\frac{\partial E}{\partial f_i}. \tag{28}$$

The partial derivatives of the equilibrium functional with respect to the macroscopic variables can be obtained as:

$$\frac{\partial f_j^{eq}}{\partial \rho} = A_j + \rho \frac{\partial A_j}{\partial \rho} + m\xi_j \frac{\partial B_j}{\partial \rho}, \tag{29a}$$

$$\frac{\partial f_j^{eq}}{\partial m} = \rho \frac{\partial A_j}{\partial m} + \xi_j B_j + \xi_j m \frac{\partial B_j}{\partial m}, \tag{29b}$$

$$\frac{\partial f_j^{eq}}{\partial E} = \rho \frac{\partial A_j}{\partial E} + \xi_j m \frac{\partial B_j}{\partial E}, \tag{29c}$$

with

$$\frac{\partial A_j}{\partial \rho} = \begin{cases} -\frac{b-1}{\eta_0^2}\frac{E\rho - 2m^2}{b\rho^3} & j = 0, \\ \frac{1}{2\left(v_1^2 - v_2^2\right)}\left(\left(\frac{v_2^2(b-1)}{\eta_0^2} + 1\right)\frac{2m^2 - E\rho}{b\rho^3} - \frac{2m^2}{\rho^3}\right) & j = 1, 2, \\ \frac{1}{2\left(v_2^2 - v_1^2\right)}\left(\left(\frac{v_1^2(b-1)}{\eta_0^2} + 1\right)\frac{2m^2 - E\rho}{b\rho^3} - \frac{2m^2}{\rho^3}\right) & j = 3, 4; \end{cases} \tag{30a}$$

$$\frac{\partial B_j}{\partial \rho} = \begin{cases} 0 & j = 0, \\ \frac{1}{2v_1^2\left(v_1^2 - v_2^2\right)}\frac{4m^2 + E\rho}{b\rho^3} & j = 1, 2, \\ \frac{1}{2v_2^2\left(v_2^2 - v_1^2\right)}\frac{4m^2 + E\rho}{b\rho^3} & j = 3, 4; \end{cases} \tag{30b}$$

$$\frac{\partial A_j}{\partial m} = \begin{cases} -\frac{b-1}{\eta_0^2}\frac{2m}{b\rho^2} & j = 0, \\ \frac{1}{2\left(v_1^2 - v_2^2\right)}\left(-\left(\frac{v_2^2(b-1)}{\eta_0^2} + 1\right)\frac{2m}{b\rho^2} - \frac{2m^2}{\rho^2}\right) & j = 1, 2, \\ \frac{1}{2\left(v_2^2 - v_1^2\right)}\left(-\left(\frac{v_1^2(b-1)}{\eta_0^2} + 1\right)\frac{2m}{b\rho^2} - \frac{2m^2}{\rho^2}\right) & j = 3, 4; \end{cases} \tag{30c}$$

and

$$\frac{\partial B_j}{\partial m} = \begin{cases} 0 & j = 0, \\ -\frac{1}{v_1^2\left(v_1^2 - v_2^2\right)}\frac{m}{b\rho^2} & j = 1, 2, \\ -\frac{1}{v_2^2\left(v_2^2 - v_1^2\right)}\frac{m}{b\rho^2} & j = 3, 4; \end{cases}$$

$$\frac{\partial A_j}{\partial E} = \begin{cases} \frac{b-1}{\eta_0^2}\frac{1}{b\rho} & j = 0, \\ \frac{1}{2\left(\nu_1^2-\nu_2^2\right)}\left(\frac{\nu_2^2(b-1)}{\eta_0^2}+1\right)\frac{1}{b\rho} & j = 1,2, \\ \frac{1}{2\left(\nu_2^2-\nu_1^2\right)}\left(\frac{\nu_1^2(b-1)}{\eta_0^2}+1\right)\frac{1}{b\rho} & j = 3,4; \end{cases} \tag{30d}$$

$$\frac{\partial B_j}{\partial E} = \begin{cases} 0 & j = 0, \\ \frac{1}{\nu_1^2\left(\nu_1^2-\nu_2^2\right)}\frac{b+2}{b\rho} & j = 1,2, \\ \frac{1}{\nu_2^2\left(\nu_2^2-\nu_1^2\right)}\frac{b+2}{b\rho} & j = 3,4. \end{cases} \tag{30e}$$

The *adjoint equilibrium distribution* can be defined as

$$\lambda_i^{eq} = \sum_{j=0}^{N-1} \frac{\partial f_j^{eq}}{\partial f_i}\lambda_j. \tag{31}$$

Now at the microscopic level, one solves the LBE to obtain solutions f_i. One then takes the moments to obtain the macroscopic variables at any time $0 \leq t \leq T$. These are then used to solve backward in time the microscopic adjoint equation (24) for the adjoint variable λ_i. The solutions thereof are used together with the optimality condition to obtain the gradient of the cost function with respect to the control $\mathbf{u}_0$.

Remark 4.1. One can derive, formally, using standard techniques, the adjoint system related to the optimization of Euler flows. The result is a backward linear system of conservation laws in the adjoint variables [26, 30].

On the other hand, moments of the adjoint Lattice Boltzmann system obtained above are considered. Applying $\sum_{i=0}^{N-1}$ to (24), leads to the equation

$$-\partial_t \Lambda - \tilde{u}\partial_x \Lambda = \frac{1}{\varepsilon}\left(\sum_{i=0}^{N-1}\lambda_i^{eq} - \Lambda\right), \tag{32}$$

where $\Lambda = \sum_{i=0}^{N-1}\lambda_i$ can be seen as an adjoint density and $\Lambda\tilde{u} = \sum_{i=0}^{N-1}\xi_i\lambda_i$ is an adjoint momentum. Similarly, one can derive an equation for the adjoint

momentum and the adjoint energy. The result is a nonlinear system of conservation laws with a source term which depends on the moments of the adjoint equilibrium distribution. Since the adjoint collision operator is a linear combination of the derivatives of the equilibrium distributions f_j^{eq} with respect to the velocity distribution f_i, the adjoint equlibrium distribution can not be chosen freely. Indeed, it was found that the adjoint equilibrium function can be expressed exactly only if the cost functional is linear in density and velocity. But this case is not of much interest in practical problems.

5 Numerical results

In the following, the numerical results that were obtained for the two previously discussed relaxation methods will be presented. All computations have been done on an Intel Centrino with 1.5 GHz.

Firstly, a brief discussion of the numerical implementation of both schemes and of the adjoint based optimization algorithm will be given. These are then applied to smooth and nonsmooth examples. It comes out that both methods are able to solve not only the smooth problems, but also the problems involving discontinuities in either the initial data $\mathbf{u}_d(x, t = 0)$ for the desired state or in the desired state $\mathbf{u}_d(x, t = T)$ itself. Finally, the sensitivity of the numerical methods presented in this paper with respect to the grid size will be considered. The results for different grid sizes for the nonsmooth example reveal that the number of iterations of the optimization algorithm is independent of the grid size that is used.

5.1 Solution of the forward and backward equations

It can be observed that, for each particle i with speed ξ_i, the Lattice Boltzmann equation (11) and its adjoint form (24) are transport equations with source terms. Therefore, they can be discretized in the finite volume framework with a second order integration in time and a second order upwind integration in space with the minmod slope limiters [32] as briefly described below. To start with the advection equation in the general form

$$\begin{cases} v_t + a v_x &= g(v), \quad (x,t) \in [0,1] \times [0,T], \\ v(x,0) &= v_0(x), \quad x \in [0,1], \end{cases} \tag{33}$$

where a is the wave speed and $g(v)$ is the source term, which is a function of the balanced quantity v is considered. A uniform grid in space $x_j = j\Delta x,\ j = 0, \ldots, K$ with the space step Δx is applied. The time grid is denoted as $t_n = n\Delta t,\ n = 0, \ldots, H$ and the time step is chosen according to the CFL condition. In the Lattice Boltzmann formulation, the Courant Number has the form

$$\mathrm{CFL} = \frac{\Delta t}{\Delta x} \max_{i=0,\ldots,N-1} \xi_i \tag{34}$$

where ξ_i are the discrete speeds. In the finite volume framework, the cell $I_j = (x_{j-1/2}, x_{j+1/2})$ where the cell boundaries are defined as $x_{j+1/2} = \frac{1}{2}(x_j + x_{j+1})$ is introduced. The cell average of the balanced quantity $v(x,t)$ for the j-th cell at time t_n is denoted as $v_j^n,\ j = 0, \ldots, K$. The considered second order scheme takes the semi-discrete form [32]

$$\frac{dv_j}{dt} = -\frac{F_{j+\frac{1}{2}} - F_{j-\frac{1}{2}}}{\Delta x} + g_j, \tag{35}$$

where g_j is the cell average of the source term and the numerical flux is given by

$$F_{j+\frac{1}{2}} = a^- v_{j+1} + a^+ v_j + \frac{1}{2}|a| \left(1 - |\frac{a\Delta t}{\Delta x}|\right) \sigma_{j+\frac{1}{2}}, \tag{36}$$

where $a^+ = \max\{a, 0\}$ and $a^- = \min\{a, 0\}$ and the slope limiters $\sigma_{j+\frac{1}{2}}$ are defined as

$$\sigma_{j+\frac{1}{2}} = \begin{cases} \mathrm{Minmod}\left(v_j - v_{j-1},\, v_{j+1} - v_j\right) & \text{if } a \geq 0, \\ \mathrm{Minmod}\left(v_{j+1} - v_j,\, v_{j+2} - v_{j+1}\right) & \text{if } a < 0, \end{cases} \tag{37}$$

with

$$\mathrm{Minmod}(x, y) = \frac{1}{2}(\mathrm{sgn}(x) + \mathrm{sgn}(y)) \cdot \min(|x|, |y|).$$

The Knudsen number is taken here as $\epsilon = 10^{-4}$ and the spatial and temporal step are chosen such that the CFL condition is satisfied. For the source term, the mid-point quadrature rule is applied. The relaxation method is implemented along the lines of [26]. Here the first-order in space and time relaxation scheme as presented for the scalar case in Section 2.1 in [23] is employed. Throughout the numerical tests the relaxation parameter is $\tau = 10^{-8}$.

Both flow solvers will be tested for the shock tube problem which can be described as follows: A tube is filled with gas and is initially divided by a

membrane into two sections. The gas on one half of the tube has a higher density and pressure than on the other one, with zero velocity everywhere. At time $t = 0$, the membrane is suddenly removed and the gas is allowed to flow. Net motion in the direction of the lower pressure is expected. Assuming uniform flow across the tube, there is variation only in one direction and the 1-D Euler equations apply. For the simulations, the initial variables are taken as

$$\mathbf{u}_0(x) = \begin{cases} (1, 0, 3) & \text{for } x < 0.5 \\ (5, 0, 15) & \text{for } x > 0.5 \end{cases} \tag{38}$$

which are compared to the exact solution computed at $t = 0.15$ on a grid of $N = 400$. The numerical solution obtained with the LBE and the relaxation method in (8) is presented in Figure 1. The solution obtained with a D1Q5 Lattice Boltzmann model produces very good results that compare well with those presented in the literature [33]. Moreover, the first-order relaxation method also gives satisfactory results.

5.2 The discrete form of the optimization problem

With the space and time discretization described above, the discrete form of the objective function can then be written as

$$\mathcal{J}(\mathbf{u}(\cdot, T), \mathbf{u}_0; \mathbf{u}_d) = \frac{\Delta x}{2} \sum_{i=1}^{K} \|\mathbf{u}_i^H - \mathbf{u}_{d\,i}\|^2.$$

Recall that the vector $\mathbf{u} = (\rho, m, E)$ contains the conservative variables which are the density, the momentum and the energy. For given initial data $\mathbf{u}_0$, one can solve the flow equations for the state variable $\mathbf{u}(\cdot, T)(\mathbf{u}_0)$ using the LBE or the relaxation method and the optimization problem (4) can be rewritten as an unconstrained minimization problem for the reduced cost functional $\tilde{\mathcal{J}}(\mathbf{u}_0, \mathbf{u}_d) = \mathcal{J}(\mathbf{u}(\cdot, T)(\mathbf{u}_0); \mathbf{u}_d)$. At each grid point the gradient of the reduced cost functional can be computed using the adjoint method: for example, from the optimality conditions, one can deduce that the gradient of the reduced cost functional for the LBE satisfies

$$\nabla_{\mathbf{u}_{0,i}} \tilde{\mathcal{J}} = \Delta x \sum_{j=0}^{N-1} \frac{\partial f_j^{eq}(\rho_0, m_0, E_0)}{\partial \mathbf{u}_{0,i}} \lambda_j(x_i, 0), \tag{39}$$

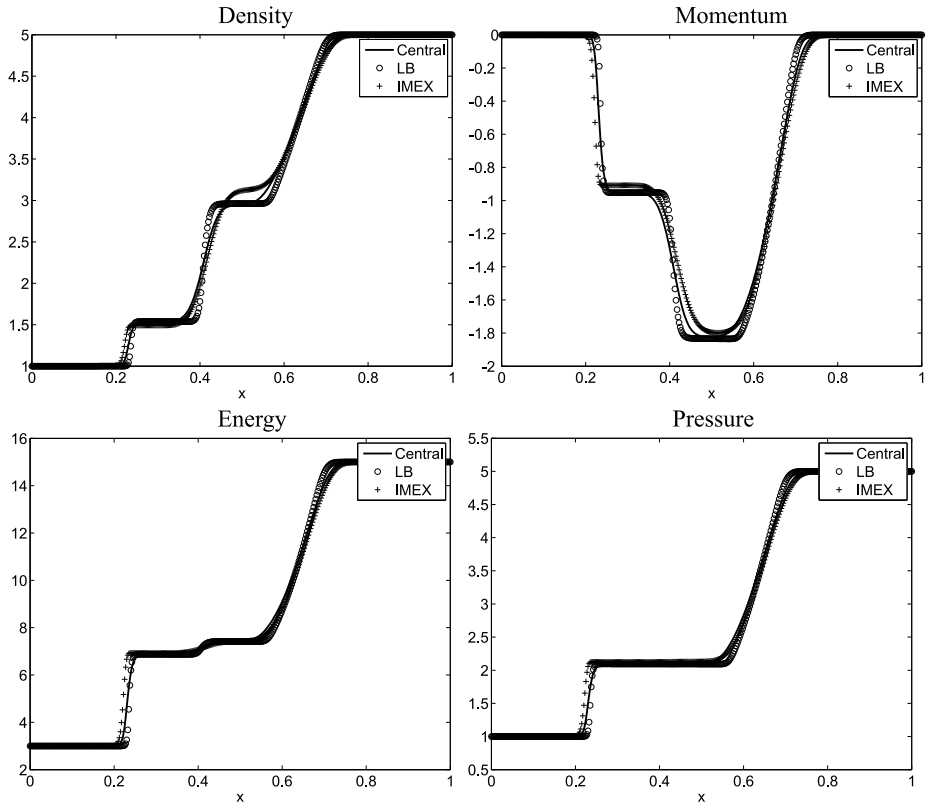

Figure 1 – Plot of the density, momentum, energy and pressure computed at time $t = 0.15$ exact (solid line), the Lattice Boltzmann method ($\circ$) and the relaxation method ($+$). The relaxation parameter is taken as $\tau = 10^{-8}$ and the Knudsen number as $\varepsilon = 10^{-4}$.

whereas for the relaxation method

$$\nabla_{\mathbf{u}_{0,i}} \tilde{\mathcal{J}} = \mathbf{p}_{0,i} + (D\mathbf{f}(\mathbf{u}_0)^T \mathbf{q}_0)_i \tag{40}$$

is obtained. Using this gradient information, the solution of the optimization problem using a steepest descent algorithm applied to the reduced cost functional $\tilde{\mathcal{J}}(\mathbf{u}_0; \mathbf{u}_d)$ is computed. Since the optimal value is known to be zero, the stopping criterion for the convergence of the optimization algorithm is taken as

$$|\tilde{\mathcal{J}}(\mathbf{u}_0, \mathbf{u}_d)| < \text{tol},$$

where $\text{tol} \ll 1$ is a predefined tolerance.

Firstly, an optimization problem constrained by a nonlinear hyperbolic system, where each equation corresponds to Burger's equation applied to the corresponding component of $\mathbf{u} = (u_1, u_2, u_3)$ is considered. The optimization problem as in (7) is solved using the IMEX scheme. The initial desired state is chosen such that the solution $\mathbf{u}_d(x, t = T)$ has various discontinuities.

5.3 Burger's equation with discontinuous desired states

For this example, the flux function of the form

$$f(\mathbf{u}) = \frac{1}{2}\left(u_1^2, u_2^2, u_3^2\right)^T$$

is considered. The spatial domain is $[0, 2\pi]$, which is discretized with $N = 300$ grid points. The time interval for this example is taken to be $[0, 2]$, which is suitably discretized such that the CFL condition is satisfied. Moreover, the desired state $\mathbf{u}_d$ is the solution at time $T = 2$ with the initial data

$$\mathbf{u}_{d,0} = \left(\frac{1}{2}\sin(x), \sin\left(\frac{\pi}{2}x\right), \frac{1}{2} + 0.03\,x + \sin(2\pi x)\right)^T.$$

The initial control for the steepest descent method is started with an initial guess of $\mathbf{u}_0 = (0.5, 0.5, 0.5)^T$. Note that the desired state consists of shock states. The numerical results for this example are presented in Figure 2. In the numerical results the relaxation method recovers the discontinuities and achieves optimality.

5.4 Euler equations with smooth desired states

A comparison of both approaches beginning with the case of smooth data in the domain $[0, 1] \times [0, T]$ will be undertaken next. Again optimal initial data such that the flow properties at time T match the desired flow properties (at time T) given by the initial data

$$\rho_{d,0}(x) = 6x^2 - 7x + 3.2,\ m_{d,0}(x) = 1.2,\ E_{d,0} = x + 1.2 \text{ for } x \in [0, 1] \quad (41)$$

is sought. The optimization algorithm will be initialised with the initial profile:

$$\rho_0(x) = 6x^2 - 7x + 3,\ m_0(x) = 1.0,\ E_0(x) = x + 1.0 \text{ for } x \in [0, 1]. \quad (42)$$

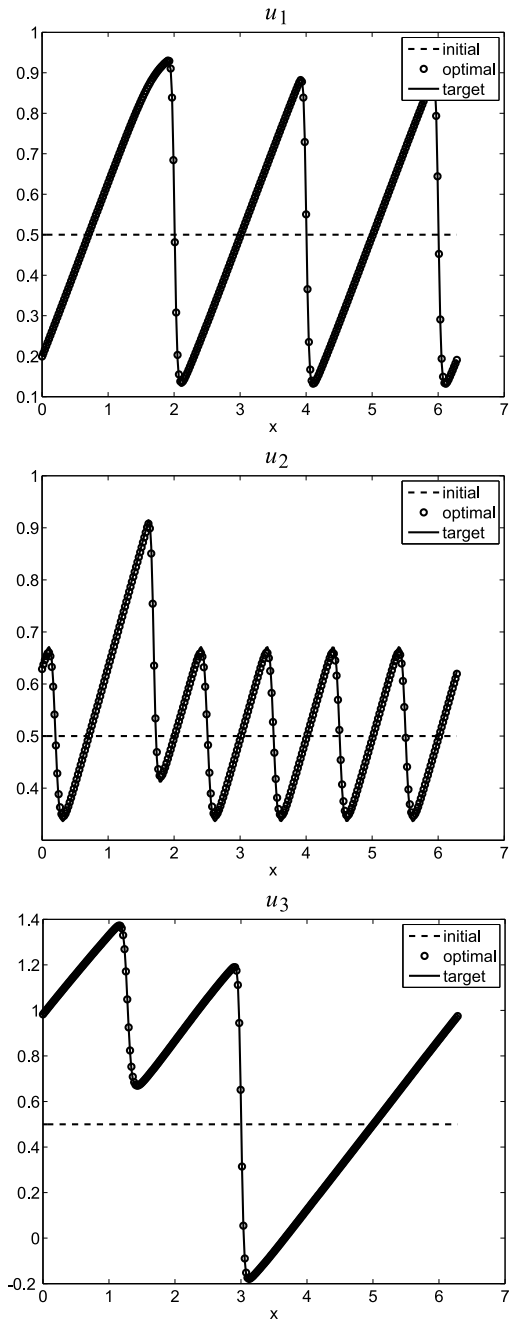

Figure 2 – Initial, optimized and target values of $\mathbf{u} = (u_1, u_2, u_3)^T$ obtained at $T = 2$ with the relaxation method for the grid size $N = 300$.

The flow equations here are solved up to time $T = 0.01$ with an optimization tolerance tol $= 10^{-4}$. The initial state computed by the optimal control approaches (initial), target and optimized states for the LBE and the relaxation method are displayed in Figure 3.

Both methods converge to the target state and optimality is achieved.

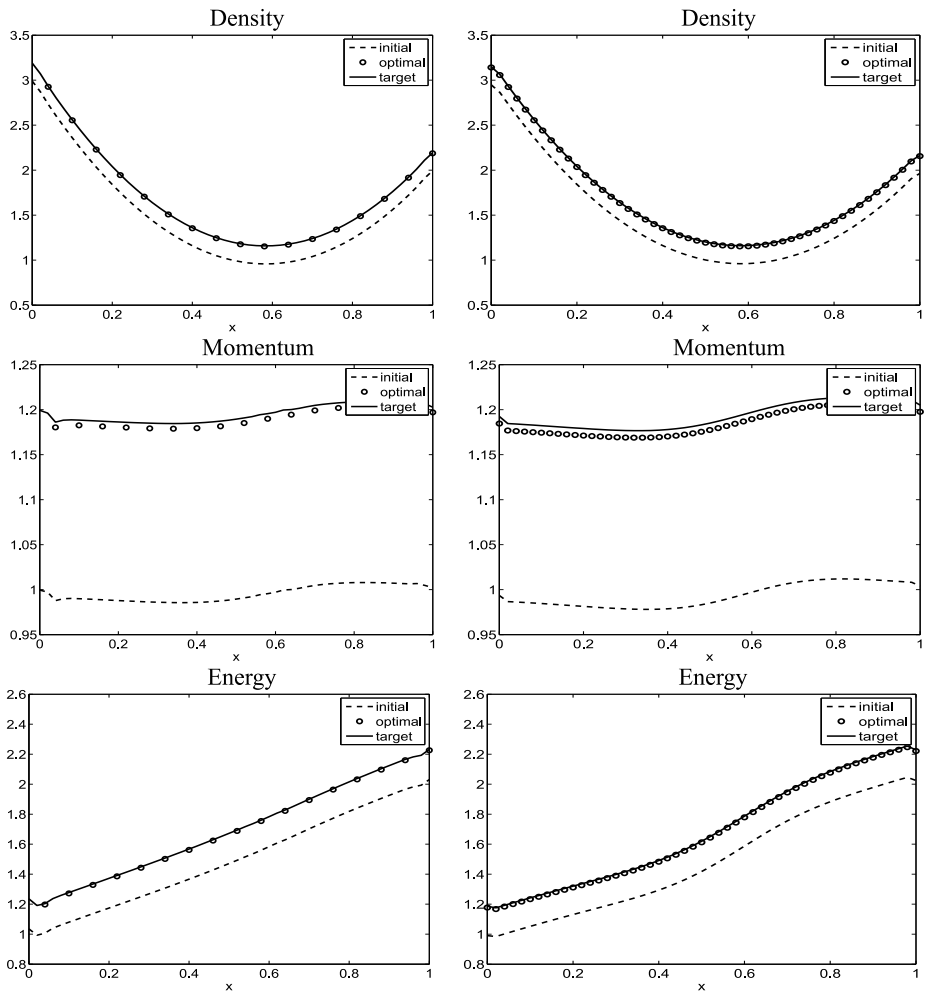

Figure 3 – Density, momentum, and energy: Initial, target and optimized values at time $T = 0.01$ for the example with smooth data obtained with the Lattice-Boltzman approach (left) and the relaxation method (right) for the grid size $N = 50$.

5.5 *Euler equations with discontinuous optimal control*

This example deals with the inverse design of a flow in a 1D shock-tube. Given a set of measurements on some actual flow at time T, the best estimate for the initial state that leads to the observed flow is determined. This problem has been explored before by many authors [30, 28, 29], but here, the linearization of the flow equation as described above and the underlying derivation of the adjoint variables for the computation of the gradient of the objective functional is used. An example taken from [34] is considered. The desired state is the solution of the Riemann problem with the initial data

$$\mathbf{u}_{d,0} = \begin{cases} (1.1,\ 0,\ 3.3), & \text{if } x < 0.5, \\ (0.2,\ 0,\ 0.6), & \text{if } x > 0.5 \end{cases} \tag{43}$$

is computed at terminal time $T = 0.03$. The state consists of different smooth and non-smooth waves.

The initial guess for the iterative optimization problem is chosen to be

$$\mathbf{u}_0 = \begin{cases} (1.0,\ 0,\ 3.0), & \text{if } x < 0.5, \\ (0.125,\ 0,\ 0.375), & \text{if } x > 0.5. \end{cases} \tag{44}$$

A tolerance of tol $= 10^{-4}$ for the optimization is prescribed. The results, using the adjoint method combined with the Lattice-Boltzmann and the relaxation approaches are presented in Figure 4. The initial control $\mathbf{u}_0$, the desired state $\mathbf{u}_d$, the optimized state and solution of the optimized flow at time T are reported in Figure 5 and it can be observed that the discontinuity is well recovered. It can also be observed that the discontinuous initial data yields several waves in the solution.

The results reveal that the approaches presented here, using the Lattice-Boltzmann model or the relaxation method, are both able to recover solutions with discontinuities such as shocks, rarefactions or contact discontinuities.

5.6 *Convergence and CPU time*

In the following, the convergence behaviour of the schemes presented in this paper is analysed. Precisely, the convergence of the optimization algorithm

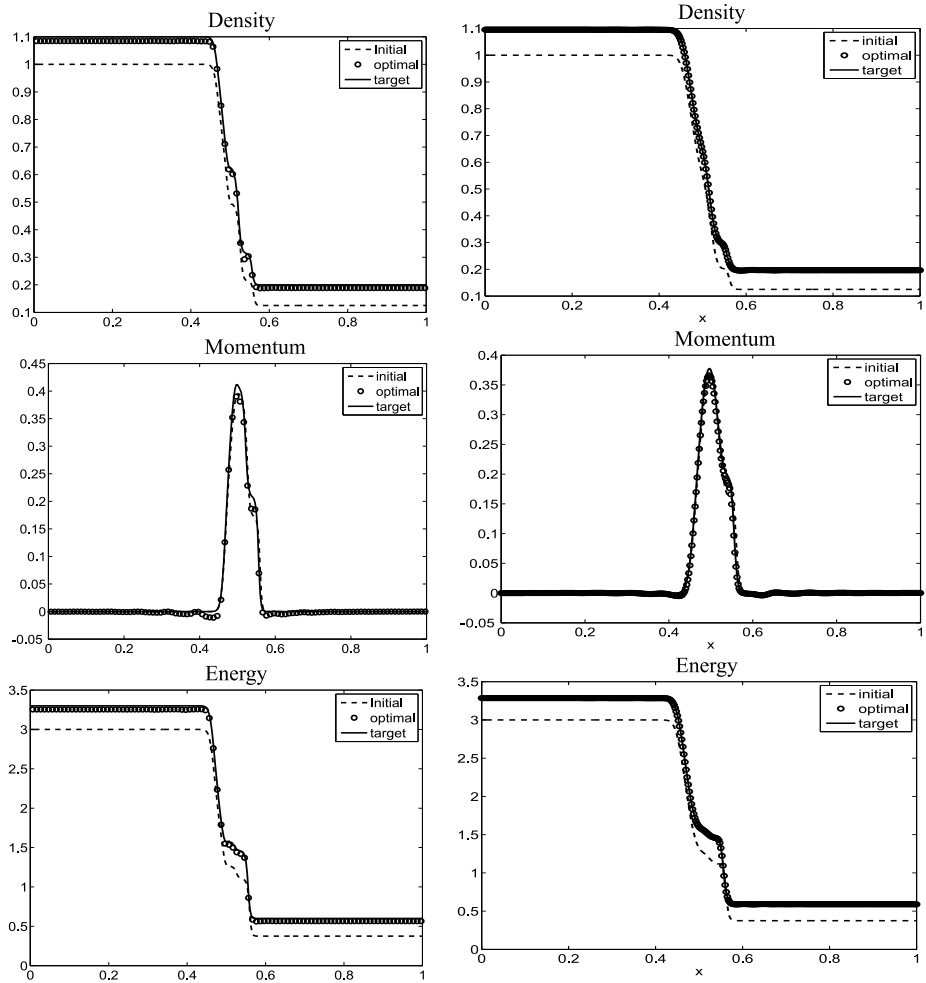

Figure 4 – Density, momentum, energy: initial, optimized and target obtained at $t = 0.03$ with the Lattice-Boltzmann method (left) on a grid with $N_x = 400$ grid points and the relaxation method (right) for a grid size of the same size.

using the Lattice Boltzmann and the relaxation approaches in terms of the number of grid points will be studied. Hence the solution for the discontinuous example presented in Section 5.5 up to tolerance tol $= 10^{-3}$ for different values of the number of discretization points $N_x \in \{50, 100, 150, 200, 250, 300\}$ is computed. In Table 1 the number of iterations obtained with the first and second order scheme for the lattice Boltzmann method, and with a first order scheme

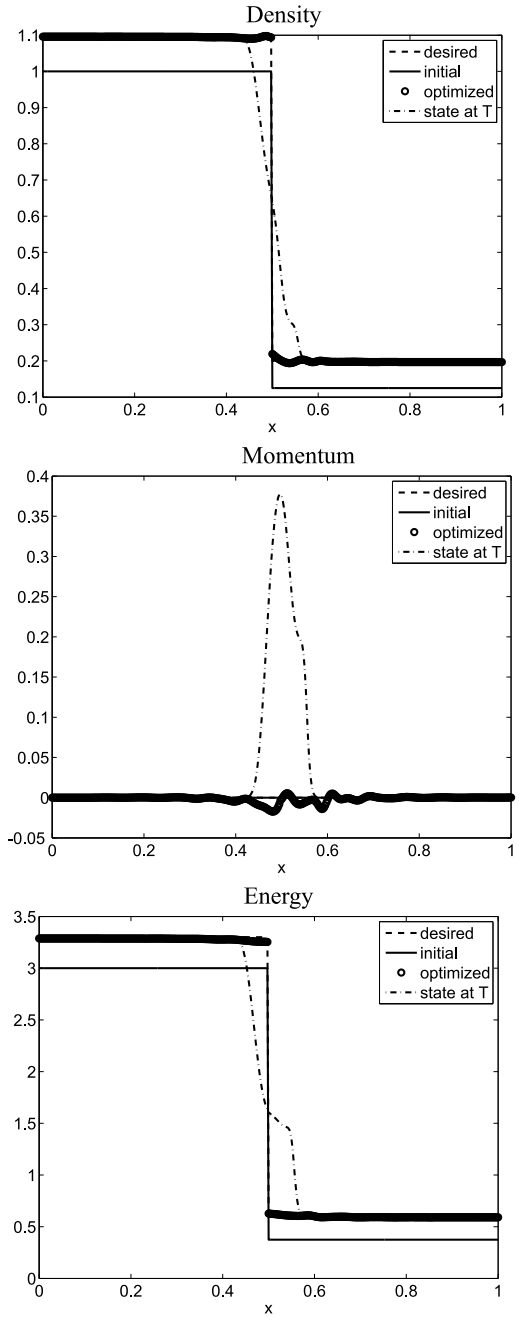

Figure 5 – Initial data, desired state, optimized state u_0 and corresponding solution at time $t = T$ to the Euler equation.

for the relaxation method, and the CPU times until convergence are presented. Note that the number of optimization iterations are independent of the grid size N_x. In Figure 6 the evolution of the cost functional as a function of the number of optimization iterations is presented. The relaxation approach converges faster than the lattice Boltzmann approach.

	LBE – 1st		LBE – 2nd		Relaxation – 1st	
N_x	It.	CPU time	It.	CPU time	It.	CPU time
50	23	3.634100e+02	23	4.179400e+02	19	1.350000e+00
100	23	5.845300e+02	23	6.931700e+02	19	2.970000e+00
150	23	8.069500e+02	23	9.692400e+02	19	5.580000e+00
200	23	1.002000e+03	23	1.246600e+03	19	8.700000e+00
250	23	1.210620e+03	23	1.527940e+03	19	1.281000e+01
300	23	1.429200e+03	23	1.793410e+03	19	1.779000e+01

Table 1 – Number of iterations (It.) and CPU times (in sec.) for the inverse design in a shock tube example obtained with the LBM and the relaxation method. Terminal time for the optimization is $T = 0.03$.

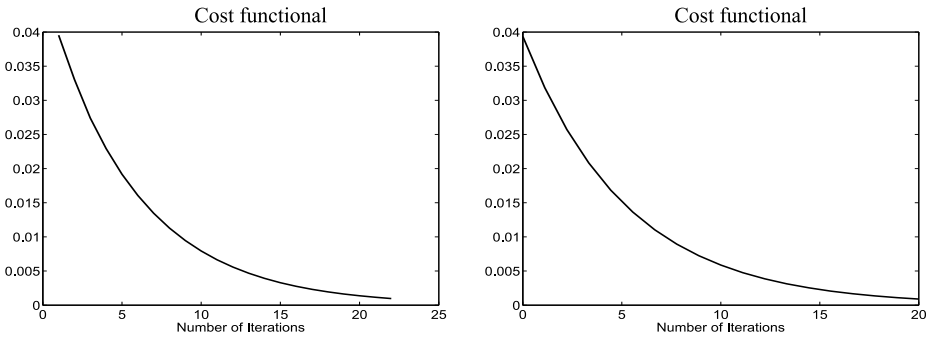

Figure 6 – Convergence history for the solution of the optimization problem computed with the LBE approach (left) and the relaxation method (right).

6 Conclusion and future work

In this paper two approaches for the control of flows governed by a system of conservation laws have been presented namely: the Lattice-Botzmann approach and the relaxation method, both combined with an adjoint calculus algorithm

for the optimization. The resulting numerical schemes perform convincingly, since they are able to handle flows with discontinuities such as shocks or contact discontinuities. Moreover, for the Euler system, the extension of the optimization methods to higher dimensions can be done. Possible difficulties would come from the boundary conditions. The multidimensional model can be used effectively to solve further interesting problems as they arise in shape optimization or topology design.

Acknowledgements. This work has been supported by DFG SPP 1253 HE-5386/8-1 and HE5386/6-1, DAAD D/08/11076 and 50727872. MKB would also like to acknowledge NRF grants (South Africa) UID 65177 and UID 61390. JMTN would like to thank the RWTH Aachen for their hospitality during a research visit there under the DAAD grant A/08/96840.

REFERENCES

[1] T. Kataoka and M. Tsutahara, *Lattice Boltzmann method for compressible Euler equations*. Physical Review, vol. E(3)69, no. 056702, (2004).

[2] S. Bianchini, *On the shift differentiability of the flow generated by a hyperbolic system of conservation laws*. Discrete Contin. Dynam. Systems, **6**(2) (2000), 329–350.

[3] A. Bressan and G. Guerra, *Shift-differentiability of the flow generated by a conservation law*. Discrete Contin. Dynam. Systems, **3**(1) (1997), 35–58.

[4] A. Bressan and M. Lewicka, *Shift differentials of maps in BV spaces*, in Nonlinear theory of generalized functions (Vienna, 1997), vol. 401 of Chapman & Hall/CRC Res. Notes Math., pp. 47–61, Chapman & Hall/CRC, Boca Raton, FL (1999).

[5] A. Bressan and A. Marson, *A variational calculus for discontinuous solutions to conservation laws*. Communications Partial Differential Equations, **20** (1995), 1491–1552.

[6] S. Ulbrich, *A sensitivity and adjoint calculus for discontinuous solutions of hyperbolic conservation laws with source terms*. SIAM J. Control Optim., **41** (2002), 740.

[7] A. Bressan and W. Shen, *Optimality conditions for solutions to hyperbolic balance laws*. Control methods in PDE-dynamical systems, Contemp. Math., **426** (2007), 129–152.

[8] F. Bouchut and F. James, *One-dimensional transport equations with discontinuous coefficients.* Nonlinear Anal., **32** (1998), 891–933.

[9] F. Bouchut and F. James, *Differentiability with respect to initial data for a scalar conservation law*, in Hyperbolic problems: theory, numerics, applications, Internat. Ser. Numer. Math, Birkhäuser, Basel (1999).

[10] F. Bouchut and F. James, *Duality solutions for pressureless gases, monotone scalar conservation laws, and uniqueness.* Comm. Partial Differential Equations, **24** (1999), 2173–2189.

[11] S. Ulbrich, *Optimal Control of Nonlinear Hyperbolic Conservation Laws with Source Terms*. Technische Universitaet Muenchen (2001).

[12] S. Ulbrich, *Adjoint-based derivative computations for the optimal control of discontinuous solutions of hyperbolic conservation laws.* Systems & Control Letters, **3** (2003), 309.

[13] Z. Liu and A. Sandu, *On the properties of discrete adjoints of numerical methods for the advection equation.* Int. J. for Num. Meth. in Fluids, **56** (2008), 769–803.

[14] C. Castro, F. Palacios and E. Zuazua, *An alternating descent method for the optimal control of the inviscid Burgers equation in the presence of shocks.* Math. Models and Meth. in Appl. Sc., **18** (2008), 369–416.

[15] C. Castro and E. Zuazua, *Systematic continuous adjoint approach to viscous aerodynamic design on unstructured grids.* AIAA Journal, **45** (2007), 2125–2139.

[16] A. Baeza, C. Carlos, F. Palacios and E. Zuazua, *2D Euler shape design on non-regular flows using adjoint Rankine-Hugoniot relations.* AIAA Journal, **47** (2009), 552–562.

[17] W.W. Hager, *Runge-Kutta methods in optimal control and the transformed adjoint system.* Numerische Mathematik, **87** (2000), 247–282.

[18] S.S. Chikatamarla and I.V. Karlin, *Lattices for the lattice Boltzmann method.* Physical Review, **E79**(046701) (2009).

[19] S.Succi, *The Lattice Boltzmann Equation for Fluid Dynamics and Beyond*. Oxford University Press (2001).

[20] S. Chen and G.D. Doolen, *Lattice Boltzmann method for fluid flows.* Annu. Rev. Fluid Mech., **30** (1998), 329–364.

[21] M.K. Banda and M. Seaid, *Higher-order relaxation schemes for hyperbolic systems of conservation laws.* J. Numer. Math, **13**(3) (2005), 171–196.

[22] M.K. Banda and M. Seaid, *Relaxation WENO schemes for multidimensional hyperbolic systems of conservation laws.* Numer. Methods Partial Differ. Equations, **23**(5) (2007), 1211–1234.

[23] S. Jin and Z. Xin, *The relaxation schemes for systems of conservation laws in arbitrary space dimensions.* Comm. Pure Appl. Math., **48** (1995), 235–276.

[24] S. Gottlieb, C.-W. Shu and E. Tadmor, *Strongly stability preserving high-order time discretization methods.* SIAM rev., **43** (2001), 89–112.

[25] L. Pareschi and G. Russo, *Implicit-explicit Runge-Kutta schemes for stiff systems of differential equations.* Recent Trends in Numerical Analysis (Eds. Brugano, Trigiante), **3** (2000), 269–284.

[26] M.K. Banda and M. Herty, *Adjoint IMEX–based schemes for control problems governed by hyperbolic conservation laws*, to appear in *Computational Optimization and Applications*.

[27] G. Pingen, A. Evgrafov and K. Maute, *Adjoint parameter sensitivity analysis for the hydrodynamic lattice Boltzmann method with applications to design optimization.* Computers and Fluid, **38** (2009), 910–923.

[28] M.D. Gunzburger, *Perspective in Flow control and Optimization*. SIAM (2002).

[29] A. Jameson, *Aerodynamic design via control theory*, in *Recent advances in computational fluid dynamics*, Springer, Berlin (1989).

[30] C. Homescu and I.M. Navon, *Optimal control of flow with discontinuities.* Journal of Computational physics, **187**(2) (2003), 660–682.

[31] P. Bhatnagar, E. Gross and M. Krook, *A model for collision processes in gases I: small amplitude processes in charged and neutral one-component systems.* Phys. Rev., **94** (1954), 511–525.

[32] R.J. LeVeque, *Finite volume methods for hyperbolic problems*. Cambridge texts in applied mathematics, Cambridge Unviversity Press (2002).

[33] R.J. LeVeque, *Numerical methods for conservation laws*. Birkhäuser Verlag (1992).

[34] M.P. Rumpfkeil and D. Zingg, *A general framework for the optimal control of unsteady flows with applications.* AIAA paper 2007–1128, (2007). 45th AIAA Aerospace Meeting and Exhibit, Reno, Nevada, USA.